

UNCLASSIFIED

AD NUMBER
AD877764
NEW LIMITATION CHANGE
TO Approved for public release, distribution unlimited
FROM Distribution authorized to U.S. Gov't. agencies and their contractors; Administrative/Operational Use; Aug 1970. Other requests shall be referred to Naval Ship Research and Development Center, Washington, DC.
AUTHORITY
USNSRDC ltr, 24 Apr 1974

THIS PAGE IS UNCLASSIFIED

TWO DIMENSIONAL SUBSONIC WIND TUNNEL TESTS ON A 20 PERCENT THICK,
5 PERCENT CAMBERED CIRCULATION CONTROL AIRFOIL

Technical Note AL-176

AD877764

AD No. _____

DDC FILE COPY

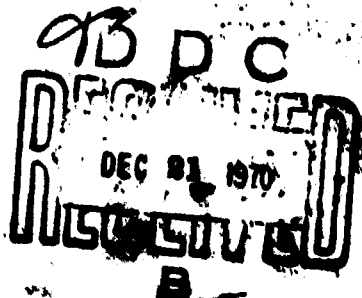
NAVY DEPARTMENT
NAVAL SHIP RESEARCH AND DEVELOPMENT CENTER
DEPARTMENT OF AERODYNAMICS
WASHINGTON, D C. ~~20007~~ 2034

TWO DIMENSIONAL SUBSONIC WIND TUNNEL TESTS ON A
20 PERCENT THICK, 5 PERCENT CAMBERED
CIRCULATION CONTROL AIRFOIL

by

Robert M. Williams and Harvey J. Howe

This document is subject to special export
controls and each transmittal to foreign
governments or foreign nationals may be made
only with prior approval of Head, Department
of Aerodynamics



August 1970

Technical Note AL-176

TWO DIMENSIONAL SUBSONIC WIND TUNNEL TESTS ON A
20 PERCENT THICK, 5 PERCENT CAMBERED
CIRCULATION CONTROL AIRFOIL

by

Robert M. Williams and Harvey J. Howe

This document is subject to special
export controls and each transmittal
to foreign governments or foreign
nationals may be made only with prior
approval of Head, Department of
Aerodynamics

August 1970

Technical Note -AL-176

TABLE OF CONTENTS

	Page
INTRODUCTION	1
MODEL AND TEST APPARATUS	1
MODEL.	1
TEST APPARATUS	2
DISCUSSION	3
DESIGN CONSIDERATIONS.	3
LIFT	4
DRAG	6
REYNOLDS NUMBER.	6
HYSTERESIS STUDY	7
EQUIVALENT LIFT-DRAG RATIO	7
LEADING EDGE SLOT.	8
REVERSE BLOWING.	8
CIRCULATION CONTROL WING	9
CONCLUSIONS.	9
REFERENCES	11

LIST OF FIGURES

	Page
Figure 1 - Detail of Cambered Circulation Control Model	12
Figure 2 - Model and Test Facility.	13
Figure 3 - Lift Coefficient Versus Momentum Coefficient for Several Angles of Attack	14
Figure 4 - Potential Flow Pressure Distributions at Zero Angle of Attack.	15
Figure 5 - Potential Flow Pressure Distributions at Three Angles of Attack.	16
Figure 6 - Variation of Drag Coefficient with Momentum Coefficient for Several Angles of Attack	17
Figure 7 - Results of Hysteresis Investigation	18
Figure 8 - Comparison of Equivalent Lift-Drag Ratios.	19
Figure 9 - Effect of a Simulated Leading Edge Slot on Performance of Basic Model	20
Figure 10 - Effect of Blowing on Lift in Reverse Flow.	21
Figure 11 - Test of Circulation Control Wing with Free Streamline Flap.	22
Figure 12 - Smoke Tunnel Photographs of Circulation Control Wing Models	23

SYMBOLS

c	chord, ft.
C_d	profile drag coefficient, e.g., Momentum deficit in wake
C_{de}	equivalent drag coefficient, $C_d + C_\mu V_j/2V_\infty$
C_ℓ	lift coefficient
C_μ	momentum coefficient, $\dot{m}V_j/qc$
C_p	pressure coefficient
D	distance between trail edge and flap, inches
d	profile drag, lbs.
d_e	equivalent drag, lbs.
h/c	dimensionless slot height
L/d_e	equivalent lift-drag ratio
\dot{m}	mass efflux, slugs/sec.
q	dynamic pressure, lbs/ft ²
r/c	dimensionless edge radius
V_j	isentropic jet velocity, ft/sec.
V_∞	freestream velocity, ft/sec.
x/c	dimensionless chordwise positions
α	angle of attack, deg
ρ	mass density of air, slugs per cubic foot

ACKNOWLEDGEMENT

The authors would like to express their sincere appreciation to Mr. Ronald Case and Mr. Van R. Olinger. Mr. R. Case conducted most of the actual testing on the cambered model. Mr. V. R. Olinger conducted the smoke tunnel studies of the circulation control wing.

SUMMARY

An experimental program has been undertaken to develop circulation control, high lift airfoils for rotary wing vehicle application. The basic method used is to eject a thin jet sheet of air tangentially over the rounded trailing edge of a thick airfoil, usually of modified elliptic cross section. The jet sheet remains attached to the rounded trailing edge, separating, eventually, on the underside. This report presents results for a twenty percent thick cambered ellipse. Lift, drag and section equivalent lift-drag ratio data are presented which indicate that this model is one of the most efficient high lift airfoils yet tested.

INTRODUCTION

A study of high lift airfoils has indicated that the method of circulation control by tangential blowing over a rounded trailing edge is more efficient than other schemes (Reference 1). The purpose of the blowing is to energize the boundary layer in order to delay separation caused by the adverse pressure gradient occurring near the trailing edge. The jet sheet remains attached due to the Coanda effect, thereby forcing the separation point around the trailing edge. In this manner a small amount of blowing causes a large change in section lift coefficient.

The present model was designed with the pressure distribution, blowing slot, and radius of the trailing edge chosen in order to optimize efficiency at zero degree angle of attack. The detailed design of this model is based on experimental and theoretical consideration discussed in References 1 and 2.

MODEL AND TEST APPARATUS

This test was conducted basically as a low speed, two-dimensional, conventional testing program. However, numerous modifications had to be made to the model, testing apparatus, and data reduction procedures to account for the peculiarities of operation at high lift.

MODEL

The model airfoil cross section was a 20 percent thick ellipse with a 5 percent circular camber line. The chord of the true 20 percent ellipse was eight inches; however, the trailing edge was rounded to a radius of 0.41 inches, which yielded an actual chord of 7.81 inches (20.5 percent thickness). An imbedded blowing slot was located at 97.3 percent chord. A slot height of 0.01 inches was used for all runs. This height was selected to maximize the jet velocity ratio V_j/V_∞ , but was also large enough to preclude choking over all but the highest values of C_u . The span of the model was the entire tunnel width, 15 inches. A detailed discussion of the effect of slot height, slot position, trailing edge radius and other effects are included in Reference 2.

A cross section of the model showing geometry and construction is shown in Figure 1. The model upper and lower surface were made of fiberglass and were joined at the leading and trailing edge with a soft epoxy

compound which facilitated alterations. The surface was finely finished using number 600 sandpaper. The upper surface was fitted with a steel blade which can be seen in a photograph of the model in Figure 2. This blade was flexed with jacking screws in order to adjust the blowing slot height. However, the blade was stiff enough that it did not distort over 15 percent under the maximum internal pressure (nominally 30 psig). The blade was undercut in order to allow the jet to leave parallel to the surface; to allow the jet to converge continuously to the slot exit and to reduce any "dead air" region occurring due to the finite blade thickness. The trailing edge incorporated a relatively large radius of curvature, $r/c = 0.041$ which was very effective in keeping the jet sheet attached. Augmentation air entered the model through both the tunnel walls by expansion cones, constructed so their terminal shape matched that of the model duct. The cones were sealed to circular plexiglass plates that allowed the angle of attack of the model to be varied. The model was in turn sealed to these rotatable end plates. Air entered equally from both ends in order to assure constant spanwise momentum distribution from the slot.

The model was fitted with two additional plenums and blowing slots, one at each end of the span, extending slightly more than one-half inch inboard. The use of the "tip jets" in retaining the two-dimensionality of the flow by controlling the tunnel wall effect is described in Reference 1.

TEST APPARATUS

The wind tunnel used for this test was the NSRDC 15 x 20 inch subsonic tunnel with a 16:1 contraction ratio. This tunnel has a partially open test section so that there was a negligible longitudinal static pressure gradient. The test section walls were made of plexiglass to permit flow visualization with tufts and oil flow. Photographs of the model installed in the test section are shown in Figure 2.

Model lift was measured by the integrated lift reaction of 46 floor and ceiling pressure taps running the entire three foot length of the test section. However, because of the far field streamline disturbance, a portion of the pressure distribution fell beyond the forward and aft taps. The amount of truncation correction was determined theoretically by the method of images to be 13 percent for all lift conditions. Conventional

solid blockage corrections were also applied to the tunnel data. No measurement of the pitching movement was attempted.

Special attention was given to the measurement of drag of the high lift model. A drag rake was preferred to a balance system for two important reasons. First, the high lift coefficients could result in a large component of induced drag that would be measured by a balance system (if the tip jets did not remove all three dimensional effects). Second because of blowing air thrust, the measured drag approached zero, which could cause inaccurate results in this range due to balance tares and hysteresis. The rake used has 55 total pressure tubes and 8 static tubes in a height of 18 inches, thus providing sufficient tube density to yield accurate results. At very high lift coefficient ($C_L \approx 6$), the wake deflection angle approached 30° (as estimated by tufts). To compensate for any angularity errors the rake was inclined 10° to the free stream. This compromise resulted in approximately five percent maximum error for both free-stream and wake readings. The method of Jones (Reference 3) was used to calculate drag from the rake data. It should be noted that a correction of $-mV_\infty$ must be added to the calculation to correct for the additional mass efflux from the jet.

Other quantities measured include model plenum pressure, temperature and mass rate of flow (calibrated for Reynolds number effects). The jet velocity, V_j , was determined by isentropic expansion from the plenum pressure to tunnel static pressure. All pressure data were recorded by a 144 tube scani-valve recorder.

DISCUSSION

DESIGN CONSIDERATIONS

The primary design consideration for this model was the generation of high lift coefficient with maximum overall efficiency. The efficiency can be described by the equivalent lift-drag ratio, $L/d_o = C_L / (C_d + C_{\mu} V_j / 2V_\infty + C_{\mu} V_\infty / V_j)$. From previous tests on several uncambered ellipse models (Reference 1) it was deduced that for low values of design lift coefficient ($C_L < 2.0$) and at low angle of attack the momentum drag, C_d , would be close to zero. Also at the corresponding low blowing coefficients the jet velocity ratio, V_j / V_∞ , would be approximately 2.0. Thus the equivalent lift-drag ratio would be near optimum when the lift augmentation ratio, C_L / C_{μ} , was maximized.

The viscous and potential flow design of the airfoil, described in Reference 2, was predicated on the above consideration. The model was actually designed for maximum lift augmentation (optimum efficiency) at zero angle of attack and lift coefficient between 1.0 and 2.0. Off design compromises necessitated by operation at other angles of attack and/or very high C_L were not considered. Lift, drag, and efficiency results are presented herein for the basic airfoil model performance tests. Results from several related tests are also presented. These include a hysteresis study, reversed flow test, leading edge slot simulation, and preliminary tests of a two-dimensional circulation control wing concept.

LIFT

The variation of lift coefficient with momentum coefficient and angle of attack is shown in Figure 3. The airfoil developed a lift coefficient of 0.5 at zero angle of attack and no blowing. With a small amount of blowing ($C_\mu = 0.05$) at zero angle of attack a lift coefficient of 3.1 was generated. This would correspond to an extremely high lift augmentation ratio of $\Delta C_L / \Delta C_\mu = 52$ for this condition. At negative angle of attack ($\alpha = -5^\circ, -10^\circ$) the augmentation ratio remained approximately the same. However, at positive angle of attack ($\alpha = +5^\circ, +10^\circ$) a sudden reduction in lift augmentation occurred. The $\alpha = +5^\circ$ condition increased initially and then abruptly changed slope while at $\alpha = +10^\circ$ the augmentation remained poor.

These seemingly anomalous results can be explained by reference to potential flow pressure distributions shown in Figure 4. The optimum slot location was determined for $\alpha = 0^\circ$ to be $x/c = 97.3$ percent for a trailing edge radius-chord ratio of 0.04 and $C_L = 1.5$. This location prevented trailing edge separation at high lift coefficient ($C_L = 3.0$) due to the extreme adverse gradient extending from $x/c = 97.5$ percent. Furthermore, the favorable gradient immediately upstream of this point insured that no upstream separation would occur. The relatively low leading edge suction pressure and moderate leading edge adverse pressure gradient were insufficient to cause a laminar bubble formation and eventual flow separation until very high lift coefficients ($C_L \sim 6$) were reached.

Again referring to the potential flow results in Figure 4, it may be seen that at low lift coefficients ($C_L \sim 1.0$) an adverse pressure gradient

extends aft of the 50 percent chord. However, the gradient does not become steep enough to cause separation until again reaching the 97.5 percent chord station so that in this case the 97.3 percent slot position was also adequate. Moreover, due to the smaller magnitude of the gradient (compared with $C_{\ell} = 3.0$ for example), the turbulent shear stress was reduced causing the coanda jet to work more efficiently. At very high values of lift coefficient ($C_{\ell} = 6$) the leading edge suction peak and adverse gradient created a small laminar separation bubble which decreased the peak suction value, thus reducing the lift and thrust contribution of the nose.

With the preceding theoretical considerations in mind the poor positive angle of attack performance can be surmised. Figure 5 shows the potential calculation for $\alpha = 10^{\circ}$. It may be readily seen that the entire airfoil was subjected to an adverse pressure gradient. Stall occurred immediately at low lift coefficient ($C_{\ell} = 1.0$). Due to this up stream separation the jet was very ineffective and generated lift augmentation only over the coanda surface at the trailing edge.

Although the model was not pressure tapped, the above description is believed accurate due to the near inviscid pressure distribution which is characteristic of circulation control airfoils. It is further validated by the drag data shown in Figure 6 and by oil and tuft observations on the model. It should be noted, however, that the model was designed for a helicopter rotor section operation at zero and slightly negative angle of attack. For operation at positive angles (an unlikely requirement), the slot would have been moved closer to the leading edge, thereby, preventing separation by the mechanisms of boundary layer control and flow entrainment, albeit at the loss of some lift augmentation and efficiency.

The maximum lift coefficient obtained is somewhat in doubt because a tunnel flow phenomena known as "incipient stagnation" (Reference 4) may have occurred. Due to the extremely large jet deflection angles generated at high lift coefficients, the jet wake partially impinged on the floor. Simultaneously, a rapid buffeting on the model occurred indicating a possible leading edge stall. If the flow impingement was sufficient, a large unsteady vortex could have periodically formed under the model also causing a buffeting. In the latter case, the measured lift would be reduced by the

low pressure vortex. This phenomena is in agreement with other studies of jet flap wings in ground effect.

DRAG

The section drag characteristics are shown in Figure 6. The data are presented for $C_d = 0.06$ and $C_\mu \leq 0.10$ where accurate integration of the wake survey is possible. At blowing coefficients greater than approximately $C_\mu = 0.10$, the wake began to impinge on the tunnel floor and partially entrained the floor boundary layer. At values of C_d above 0.06, the wake filled the entire rake. Both of these considerations made it difficult to determine drag precisely beyond their respective limitations.

It can be noted that the airfoil exhibits very low, even negative, drag coefficients in the design range (i.e., $1.0 \leq C_L \leq 2.0$; $-5^\circ \leq \alpha \leq 0$; corresponding to $.005 \leq C_\mu \leq .03$). The thrust recovery factor, $\Delta C_d / \Delta C_\mu$ gradually decreased with blowing. This phenomena was probably due to a rapid initial reduction in separation drag (base pressure drag) followed by increasing mixing losses and lower wake energy levels associated with the higher jet detachment angles. If the detachment angle were fixed by a vane or small radius trailing edge the jet sheet would leave the model with a higher energy level and hence would exhibit even greater thrust recovery (as in a blown flap), albeit at the loss of lift augmentation.

The model was tested at a Reynolds number of 560,000, characteristic of a rotor or low speed wing. It is likely that at low lift coefficients the transition point may have varied. However at $C_L > 3.0$ oil studies indicated a small laminar bubble formation which would force transition at the leading edge. This phenomena also reduced the peak suction thereby reducing the suction thrust.

REYNOLDS NUMBER

Two Reynolds number, 560,000 and 890,000, were run at zero angle of attack. No differences were observed in the C_L versus C_μ relationship. This is not to suggest, however, that there is no Reynolds number effect present but rather, that no significant effect occurred in the rather small testing range available in the wind tunnel. Certainly the energy content of the upstream boundary layer should have an important influence

on the blowing requirement. Furthermore, the coanda separation is largely influenced by the lower surface separation location and separation bubble pressure. Significant Reynolds number effects on other models are discussed in Reference 2.

Oil flow studies showed a clearly defined laminar separation bubble occurring at the leading edge only about one percent chord in length. This would be expected at high lift coefficient where the sharp suction peak and adverse pressure gradient occurred (Figure 4). The flow appeared to reattach as a turbulent boundary layer after this point (noted by a thinning of the oil film). It is therefore quite likely that over most of the lift coefficient range the upper surface boundary layer was turbulent from about 5 percent chord aft.

HYSTERESIS STUDY

Previous investigations of uncambered 20 percent ellipsis (Reference 1) have noted that various types of flow separation can occur depending on the angle of attack and blowing coefficient. For example, at fixed angle of attack with increasing blowing, a leading edge stall would occur due to a bubble formation. However at constant blowing and increasing angle of attack a thick airfoil type stall occurred. In order to quantitatively study these phenomena the present model was tested both ways. The cross-plotted results shown in Figure 7 indicate that no important hysteresis effect exists on this particular model.

A more classical type of hysteresis also considered possible was simply a "loop" in the C_L versus α curve. This phenomena was not noticed implying that the jet sheet has a strong stabilizing effect on the flow even under separated conditions.

EQUIVALENT LIFT-DRAG RATIO

In order to properly compare this airfoil with other high lift devices it is necessary to compute the total power requirement or efficiency. The use of an equivalent lift-drag ratio is proposed, herein, for all future airfoil comparisons. The equivalent drag is defined as follows:

$$d_e = d + \Delta V_j^2 / 2V_\infty + \Delta V_\infty$$

Where d is the momentum deficit measure in the wake and $\dot{m}V_j^2/2V_\infty$ is the kinetic energy flux from the nozzle and expanded to freestream velocity.

The third term, $\dot{m}V_\infty$, represents a momentum drag which could be incurred when bringing the freestream into an air intake. This term is actually pessimistic because an actual aircraft would not necessarily have to pay this "ram drag" penalty, i.e., the air could enter the intake at considerably lower velocity than that which the section experiences.

In terms of dimensionless coefficient the equivalent lift-drag ratio is given by:

$$l/d_e = C_L / (C_d + C_\mu V_j^2 / 2V_\infty + C_\mu V_\infty / V_j)$$

This ratio is plotted in Figure 8 against section lift coefficient for three angles of attack ($-5 \leq \alpha \leq +5$). It may be seen that maximum values of about $l/d_e = 90$ at lift coefficients of 1.5 are developed. These results are very significant in that they are far superior to other high lift airfoil systems (Reference 1). Furthermore, the results are very competitive with lift-drag ratios of conventional rotor sections such as the NACA 0012 airfoil operating at lower lift coefficients.

LEADING EDGE SLOT

The effect of a raised, 0.01 inch simulated slot at the leading edge was investigated briefly. Figure 9 shows the test results where the primary effect was to decrease the lift with no blowing. This would imply that an imbedded slot configuration without any abrupt curvature changes would be necessary to prevent a lift loss in reverse flow if a rotor with leading and trailing edge slots were used.

REVERSE BLOWING

The airfoil was tested in a reverse flow condition at zero angle of attack as shown schematically in Figure 10. With zero blowing, a lift coefficient of approximately 0.24 was developed, similar to the leading edge trip tests. With increasing blowing, a highly non-linear lift variation developed, gradually decreasing in magnitude.

CIRCULATION CONTROL WING

To investigate the feasibility of a high lift wing section, a model with a 15 percent chord trailing edge flap was tested. The flap was arranged in such a manner as to float behind the wing in line with the local free streamline. It was intended as a high speed fairing which truncated the airfoil to help keep the center of pressure forward. The spacing between the trailing edge and the flap was varied in order to determine its effect on the entrainment of air around the rounded trailing edge. Figure 11 shows the results of these tests where it may be seen that definite flap proximity effects occurred and were minimized only by an impractically large displacement of the flap position.

These results implied that the flap should be retracted into the airfoil rather than displaced from the trailing edge. Several methods of achieving this effect are currently under study. One of these, a "split coanda flap", is shown in smoke flow in Figure 12. Two trailing edge radii corresponding to 4 percent and 8 percent of chord were studied. The 8 percent radius exhibited a strong up flow which implied a considerable reduction in lower surface pressure resulting in reduced lift augmentation. The 4 percent radius gave higher lift augmentation and hence was selected for further study.

CONCLUSIONS

- A circulation control airfoil for helicopter rotors has been tested which generated very high equivalent lift drag ratios at lift coefficients from 1.0 to 2.0. This performance is believed superior to all other current high lift systems.

- A maximum section lift coefficient of 6.30 was obtained for a blowing coefficient of 0.23 thus demonstrating higher lift augmentation than previously obtained.

- The airfoil operated very satisfactorily at its design angle of attack, $\alpha = 0^\circ$, and negative angles of attack. At positive angles a flow separation occurred due to the extreme aft slot position. This separation seriously degraded the airfoil performance so that operation in this range was not advantageous with this slot position.

- Initial investigations of a high lift wing section substantiate the feasibility of wing circulation control but indicate a retractible type trailing edge is preferable to a "free floating" flap. .

Department of Aerodynamics
Naval Ship Research and Development Center
Washington, D. C. 20034
August 1970

REFERENCES

1. Williams, Robert M. Some Research on Rotor Circulation Control. In CAL/AVIABS Symposium on Aerodynamics of Rotary Wing and V/STOL Aircraft. 3rd, Buffalo, Jun 1969. Proceedings, Vol. 2
2. Williams, Robert M. Design Considerations of Circulation Control Airfoils. (Naval Ship Research and Development Center. Technical Note AL-185 (To be published)
3. Schlichting, Hermann. Boundary-Layer Theory. 6th ed. N.Y., McGraw-Hill 1968.
4. Lazzaroni, F. A. and L. W. Carr. Problems Associated With Tunnel Tests of High Disk Loading Systems at Low Forward Speeds. In CAL/AVIABS Symposium on Aerodynamics of Rotary Wing and V/STOL Aircraft. 3rd, Buffalo, Jun 1969. Proceedings, Vol. 2

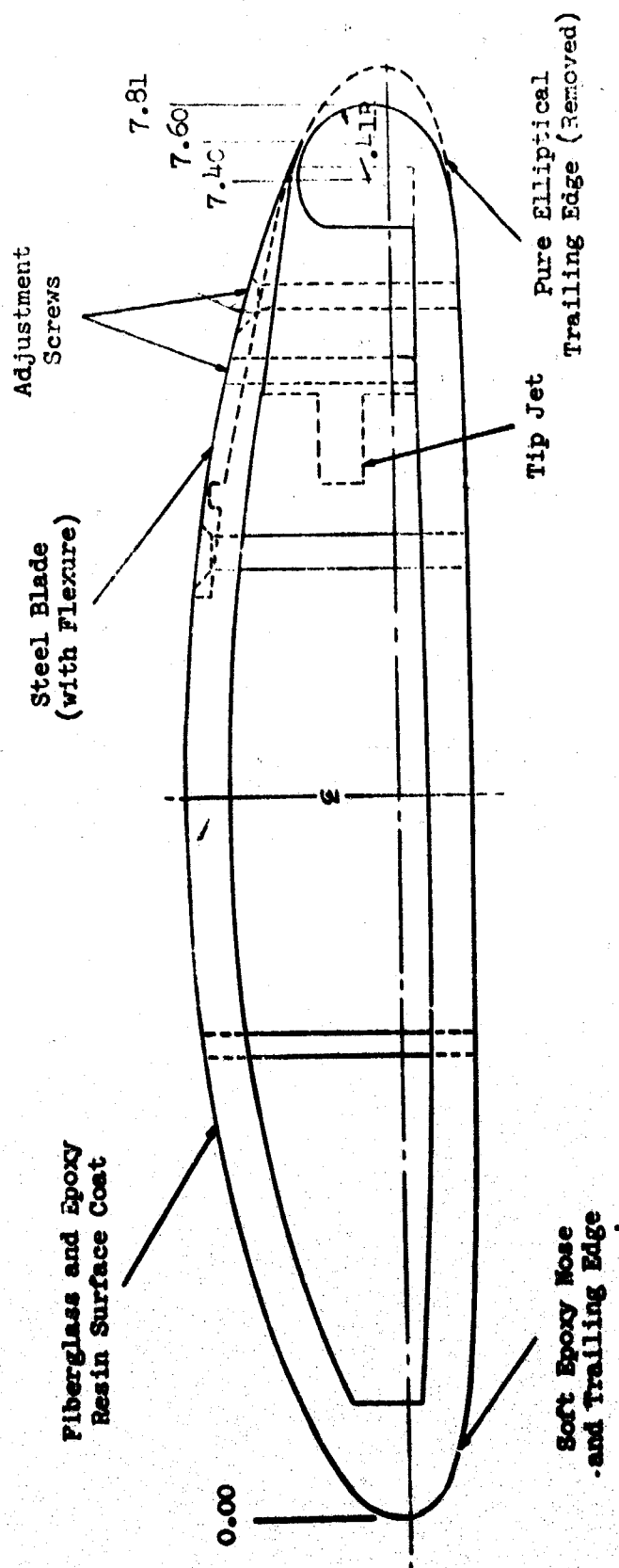
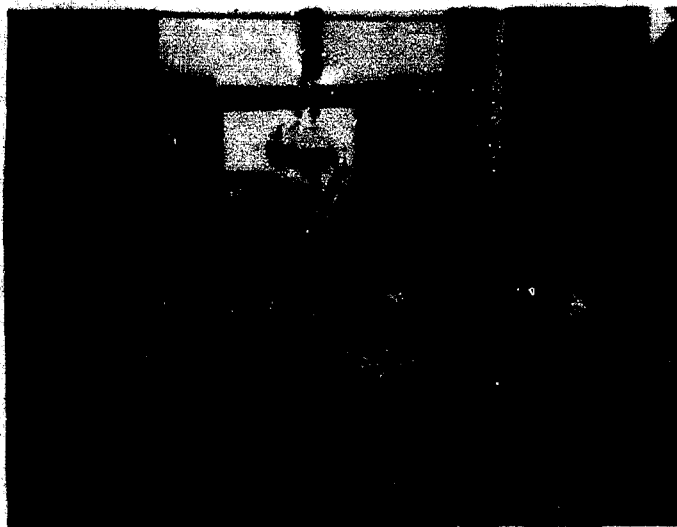


Figure 1 - Detail of Cambered Circulation Control Model



(a) Two Dimensional Wind Tunnel Facility



**(b) Model Showing Metal Blade Slot and
Tip Jets**

Figure 2 - Model and Test Facility

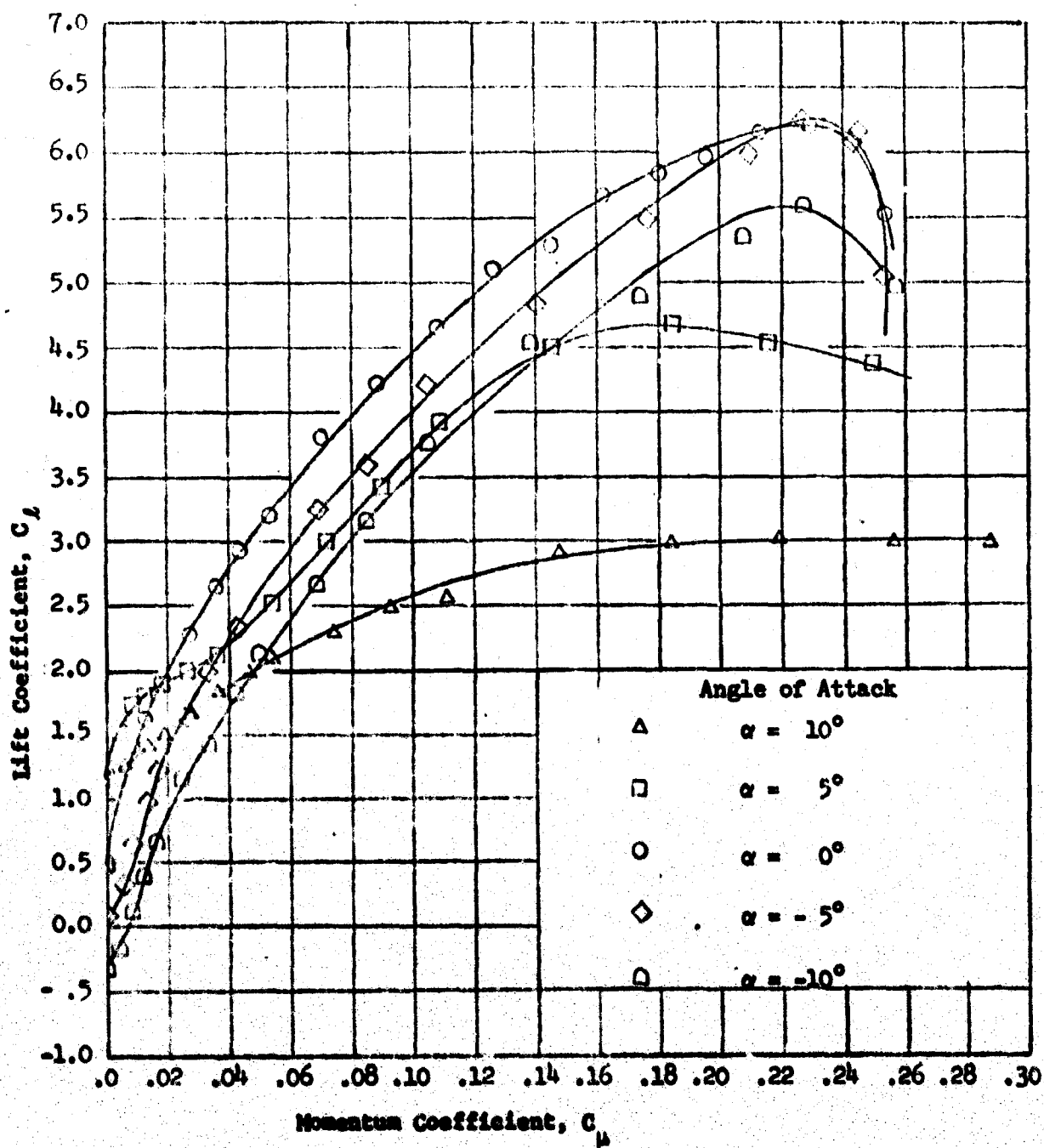


Figure 3 - Lift Coefficient Versus Momentum Coefficient for Several Angles of Attack

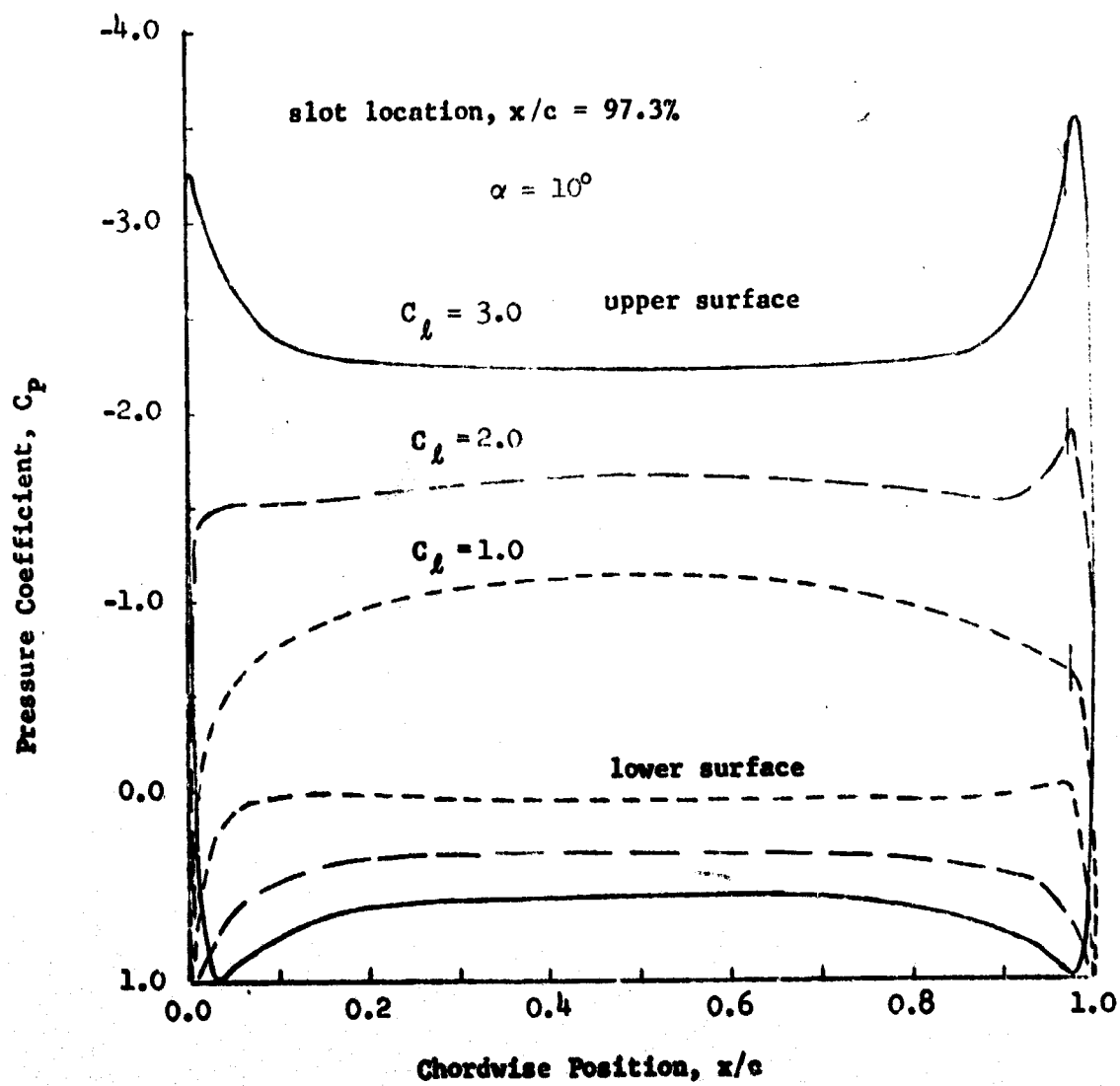


Figure 4 - Potential Flow Pressure Distributions
at Zero Angle of Attack

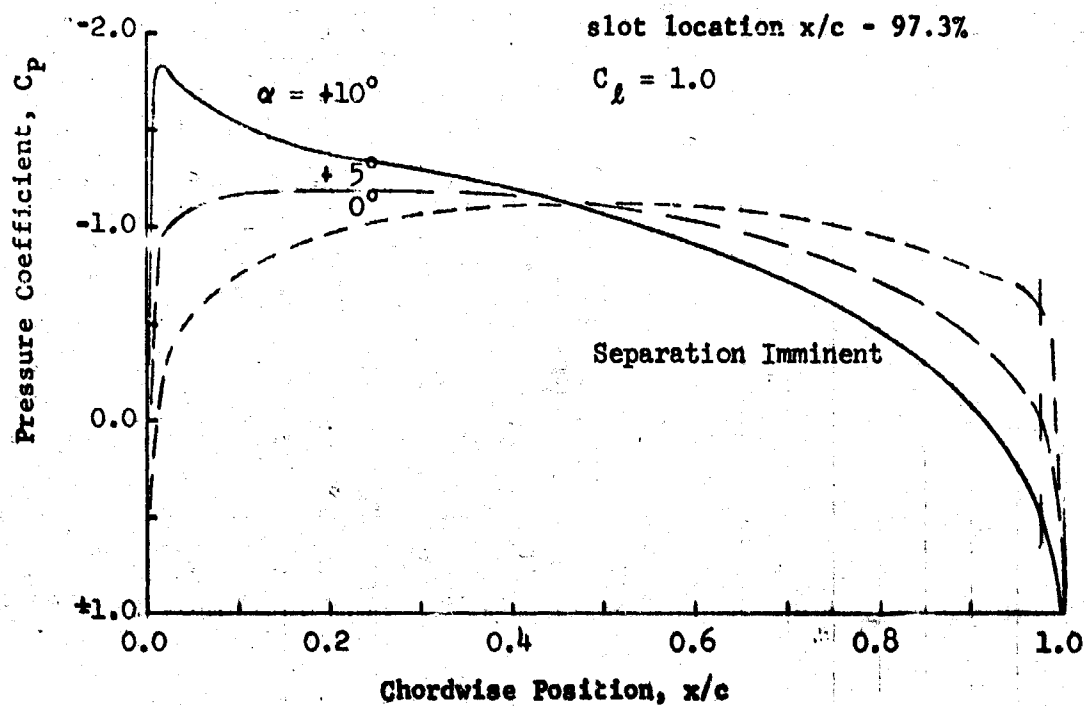


Figure 5 - Potential Flow Pressure Distributions
 at Three Angles of Attack

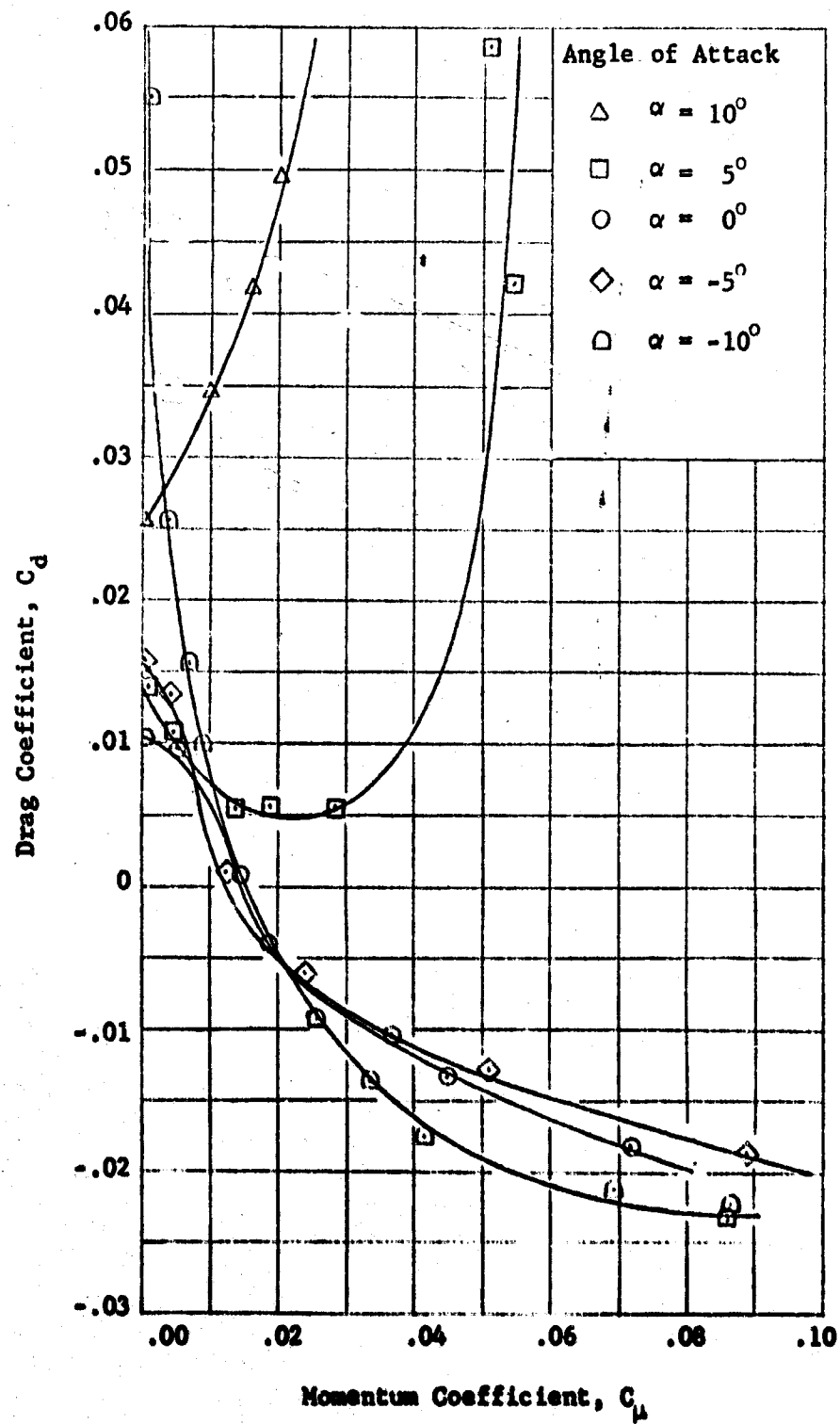


Figure 6 - Variation of Drag Coefficient with Momentum Coefficient for Several Angles of Attack

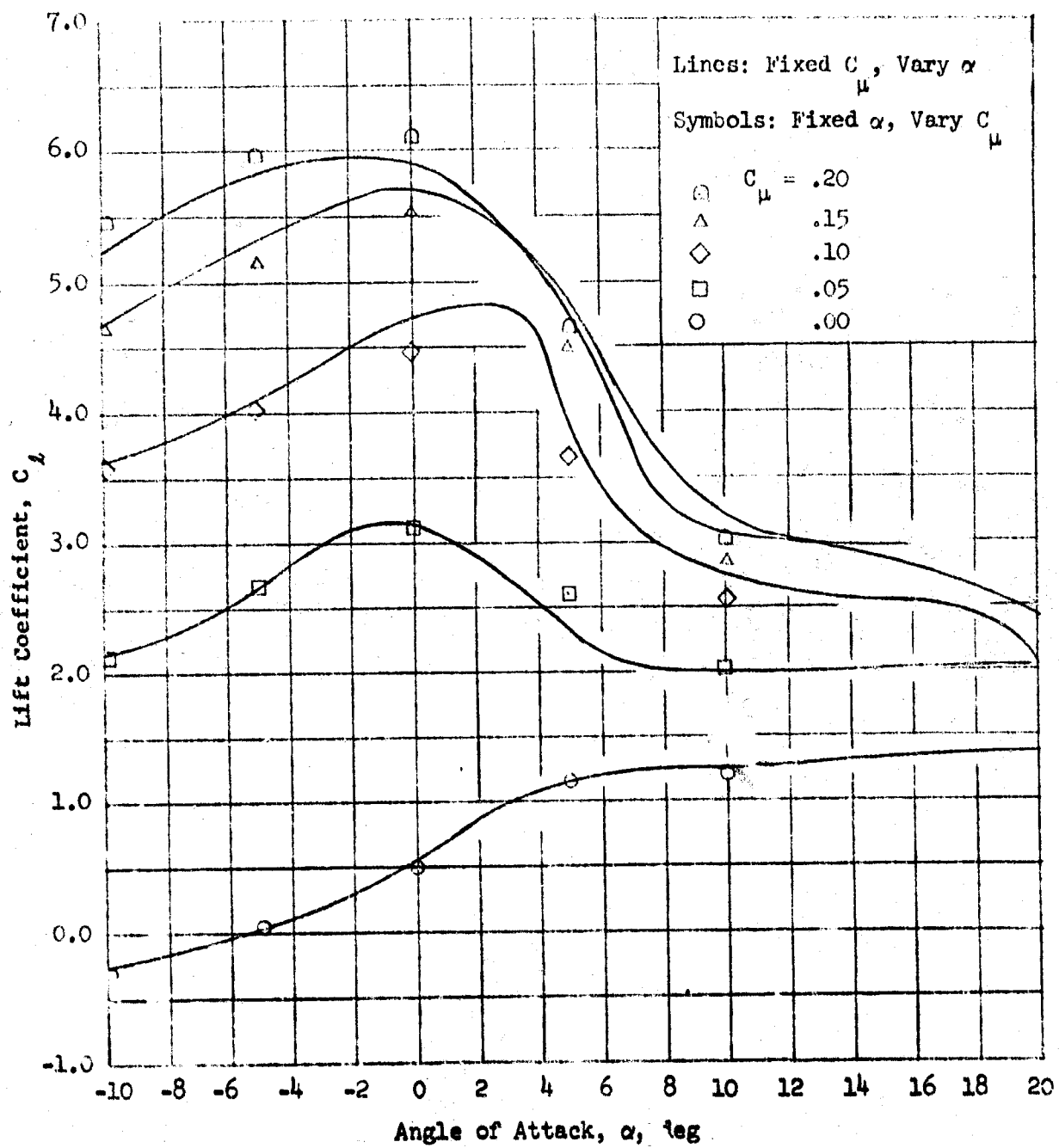


Figure 7 - Results of Hysteresis Investigation

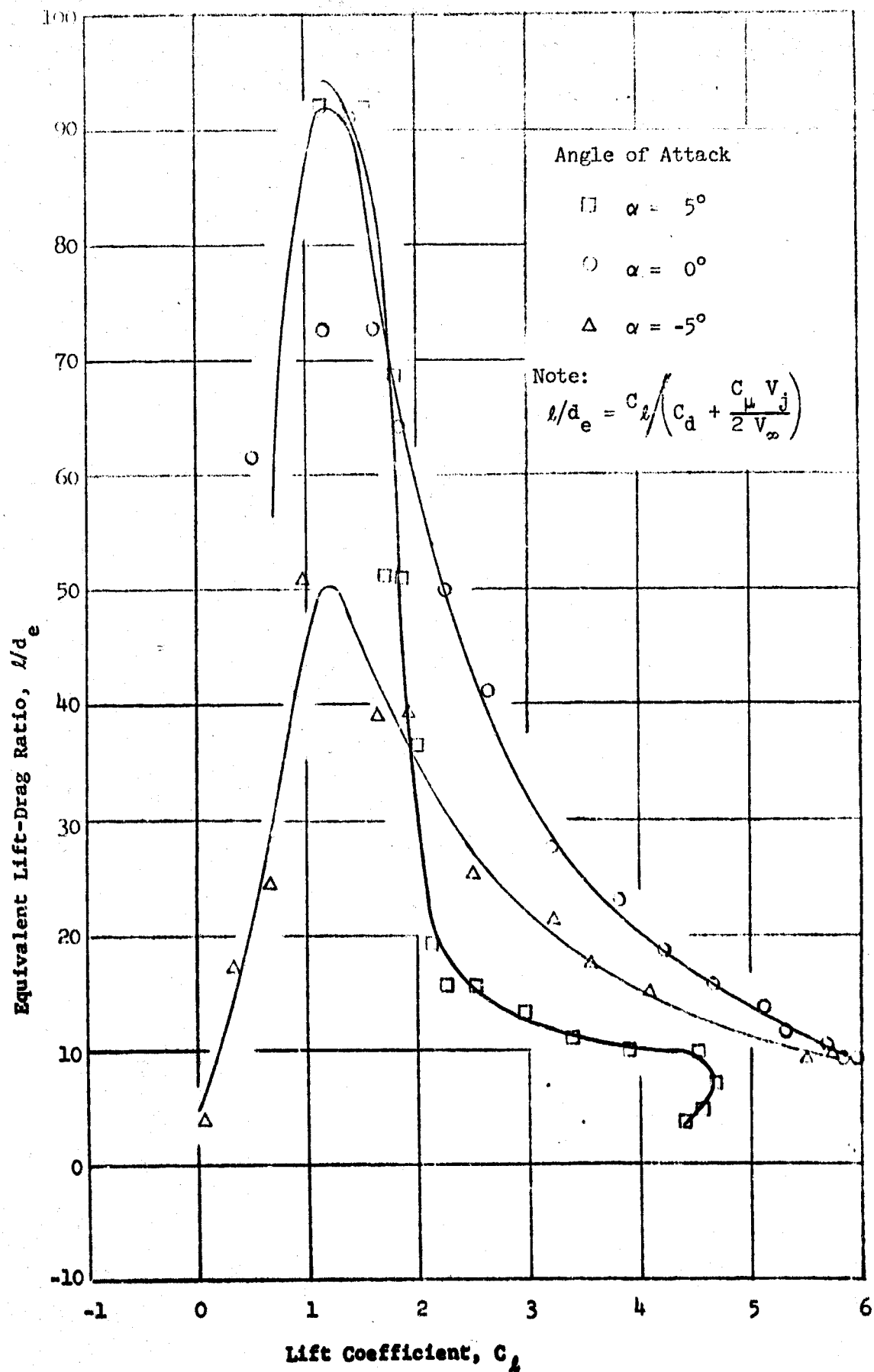


Figure 8 - Comparison of Equivalent Lift-Drag Ratios

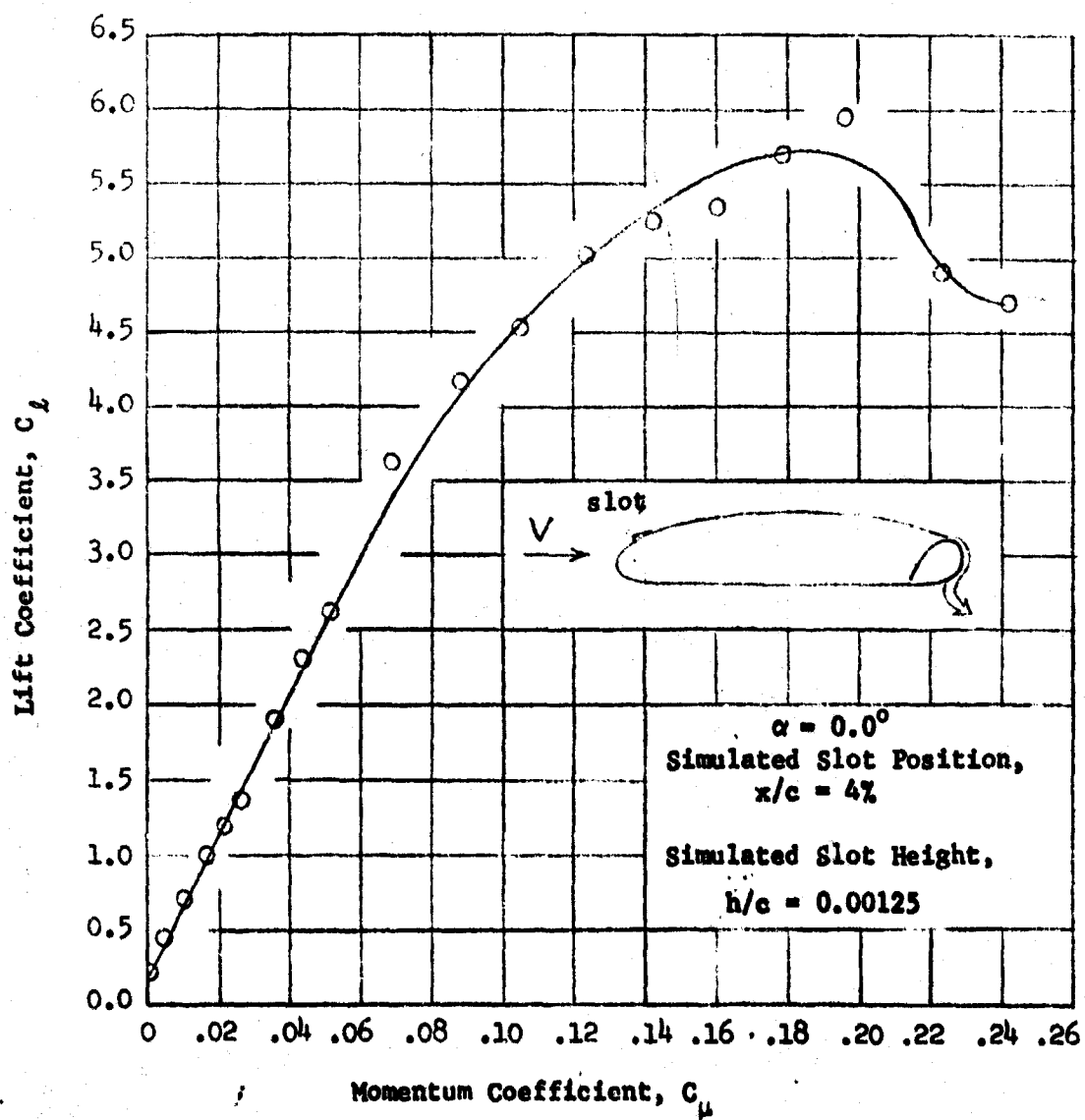


Figure 9 - Effect of a Simulated Leading Edge Slot on Performance of Basic Model

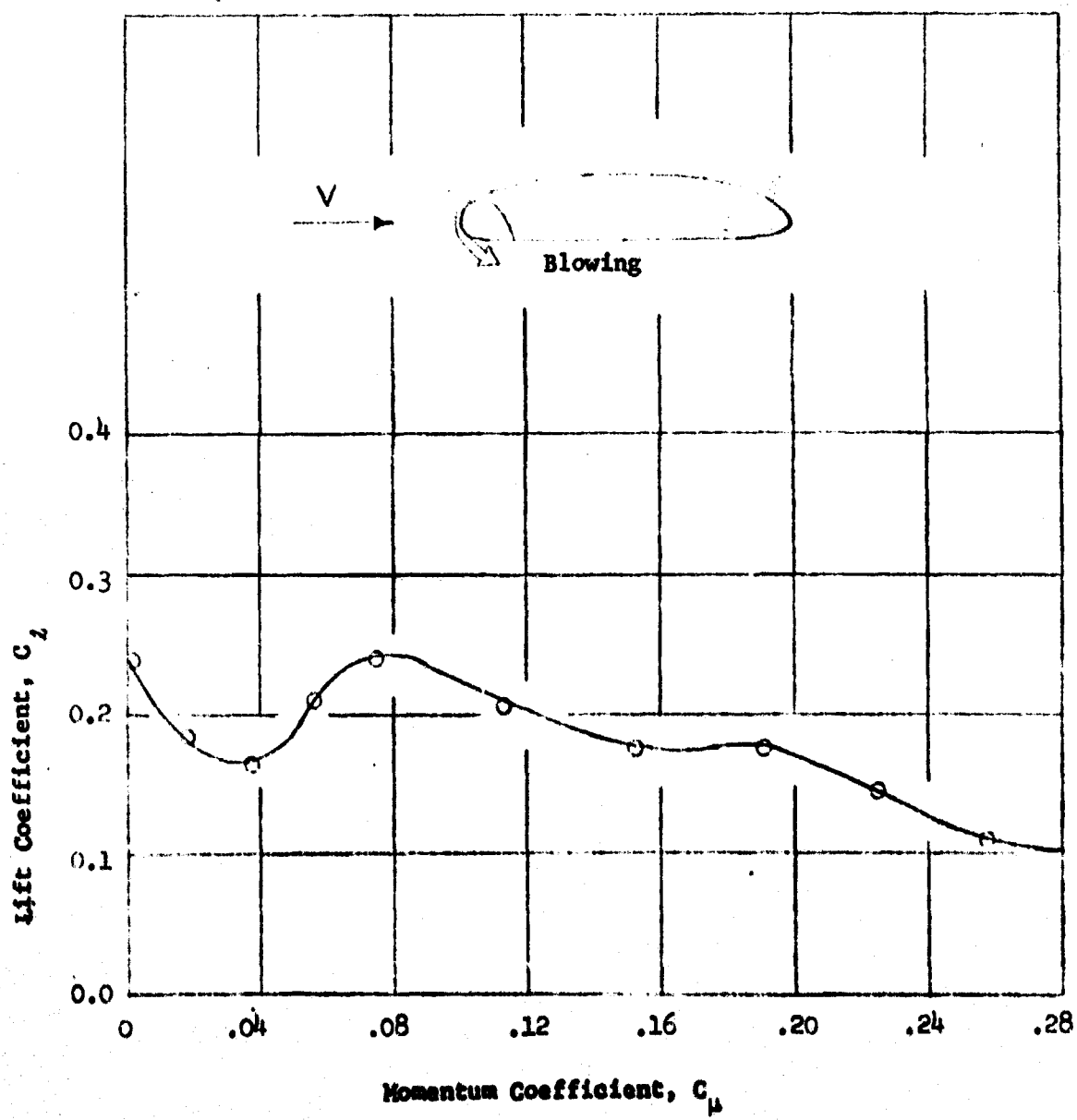


Figure 10 - Effect of Blowing on Lift in Reversed Flow

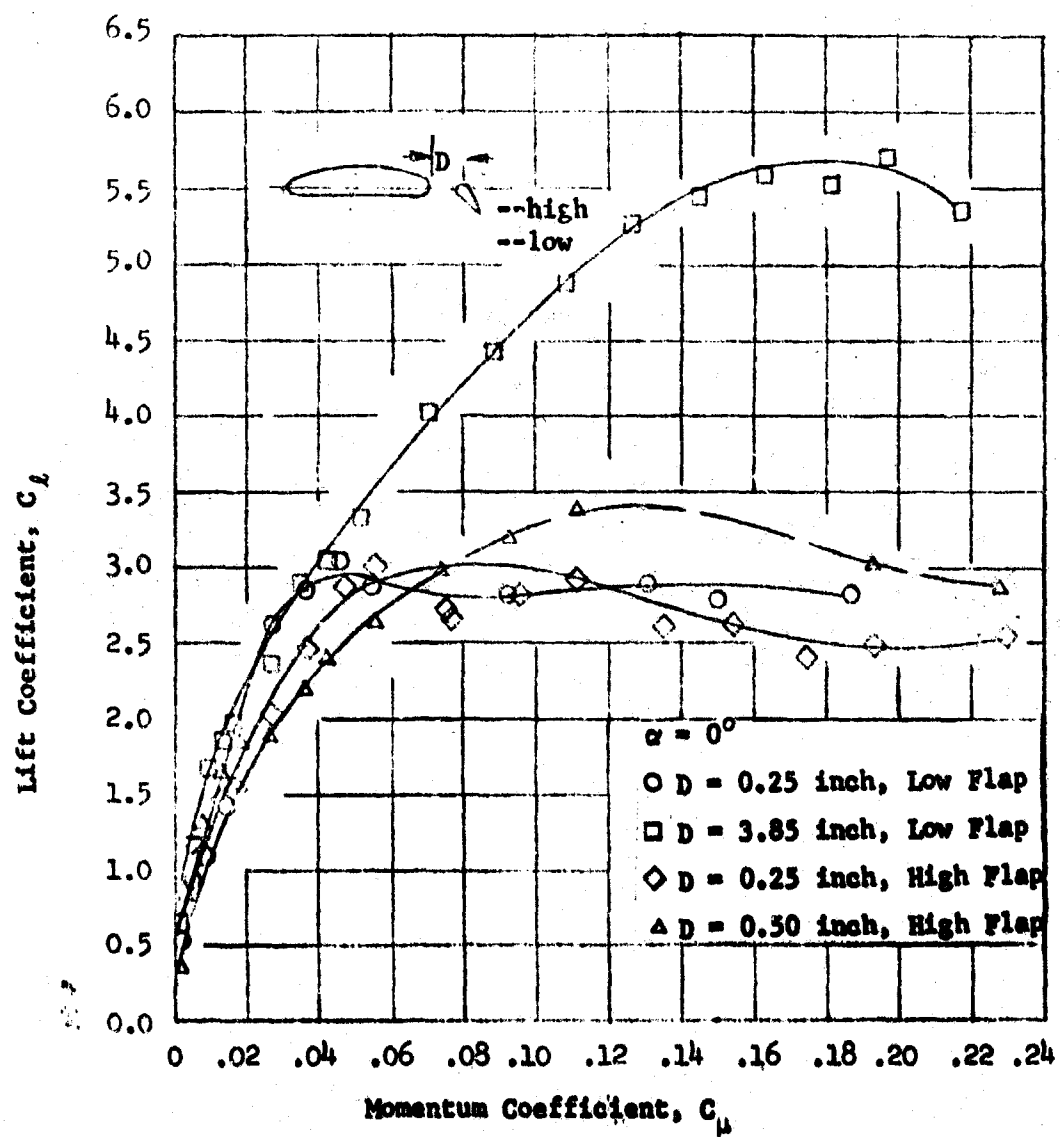
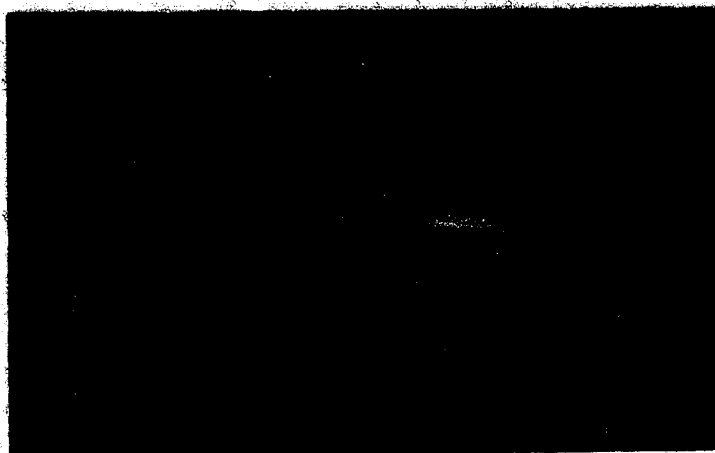


Figure 11 - Tests of Circulation Control
Wing with Free Streamline Flap



(a) Four Percent Trailing Edge Radius/Chord, Drooped
Leading Edge, $C_l \approx 4.5$



(b) Eight Percent Radius/Chord, 35° Drooped
Leading Edge, $C_l \approx 4.9$

Figure 12 - Smoke Tunnel Photographs of Circulation
Control Wing Models

UNCLASSIFIED

Security Classification

DOCUMENT CONTROL DATA - R & D

(Security classification of title, body of abstract and indexing annotation must be entered when the overall report is classified)

1. ORIGINATING AGENCY (Corporate author)		2b. REPORT SECURITY CLASSIFICATION	
Department of Aerodynamics Naval Ship Research and Development Center Washington, D.C. 20034		Unclassified	
3. REPORT TITLE			
TWO DIMENSIONAL SUBSONIC WIND TUNNEL TESTS OF A 20 PERCENT THICK, 5 PERCENT CAMBERED CIRCULATION CONTROL AIRFOIL			
4. DESCRIPTIVE NOTES (Type of report and inclusive dates)			
Technical Note			
5. AUTHOR(S) (First name, middle initial, last name)			
Robert M. Williams and, Harvy J. Howe			
6. REPORT DATE	7a. TOTAL NO. OF PAGES	7b. NO. OF REFS	
August 1970	23	3	
8a. CONTRACT OR GRANT NO.	9a. ORIGINATOR'S REPORT NUMBER(S)		
b. PROJECT NO ZR011 0101	Technical Note AL-176		
c.	9b. OTHER REPORT NO(S) (Any other numbers that may be assigned this report)		
d. NSRDC 635-673			
10. DISTRIBUTION STATEMENT			
This document is subject to special export controls and each transmittal to foreign governments or foreign nationals may be made only with prior approval of Head, Department of Aerodynamics.			
11. SUPPLEMENTARY NOTES		12. SPONSORING MILITARY ACTIVITY	
		Naval Material Command (0314) Washington, D.C. 20360	
13. ABSTRACT			
<p>An experimental program has been undertaken to develop circulation control, high lift airfoils for rotary wing vehicle application. The basic method used to eject a thin jet sheet of air tangentially over the rounded trailing edge of a thick airfoil, usually of modified elliptic cross section. The jet sheet remains attached to the rounded trailing edge, separating, eventually, on the underside. The present report presents results for cambered ellipse. Lift, drag and section equivalent lift-drag ratio data are presented which indicate that this model is one of the most efficient high lift airfoils yet tested. ()</p>			

Security Classification

DD FORM 1473 (BACK)
(PAGE 2)

UNCLASSIFIED
Security Classification